

SHORT COMMUNICATION

Muscle fibers bear a larger fraction of passive muscle tension in frogs compared with mice

Gretchen Meyer¹ and Richard L. Lieber^{2,*}**ABSTRACT**

Differences in passive muscle mechanical properties between amphibians and mammals have led to differing hypotheses on the functional role of titin in skeletal muscle. Early studies of frog muscle clearly demonstrated intracellular load bearing by titin, but more recent structural and biological studies in mice have shown that titin may serve other functions. Here, we present biomechanical studies of isolated frog and mouse fibers, and fiber bundles to compare the relative importance of intracellular versus extracellular load bearing in these species. Mouse bundles exhibited increased modulus compared with fibers on the descending limb of the length–tension curve, reaching a 2.4-fold elevation at the longest sarcomere lengths. By contrast, frog fibers and bundles had approximately the same modulus at all sarcomere lengths tested. These findings suggest that in the mouse, both muscle fibers and the ECM are involved in bearing whole muscle passive tension, which is distinct from the load bearing process in frog muscle, where titin bears the majority of whole muscle passive tension.

KEY WORDS: Muscle mechanics, Passive stiffness, Comparative biomechanics, Titin

INTRODUCTION

Mechanical properties of skeletal muscle, specifically length–tension and force–velocity relationships, were first elucidated in frog skeletal muscle (Edman, 1966; Gordon et al., 1966a; Hill, 1938, 1953). Frog muscle provides a clear experimental advantage over mammalian muscle: the ability to dissect individual, intact muscle fibers from tendon to tendon, enabling study of the smallest intact muscle unit that includes both the excitation and contraction systems. Thus, our detailed knowledge of muscle mechanics is largely based on high-resolution experiments, performed several decades ago, on isolated intact frog muscle fibers (Edman, 1979; Gordon et al., 1966b).

A seminal discovery made in frog muscle was that most of the passive load-bearing structures were intracellular and distinct from the extracellular matrix (ECM) (Magid and Law, 1985). This finding led to the identification and detailed studies of the giant intramuscular protein titin (also called connectin; Horowitz et al., 1986; Maruyama et al., 1984). Titin plays several key biological and mechanical roles in skeletal muscle, including stabilizing the

A-band at the center of the sarcomere (Horowitz et al., 1986), providing a template for sarcomere structure (Labeit and Kolmerer, 1995), stretch-dependent signaling (Knöll et al., 2002; Lange et al., 2005) and regulation of myosin filament length (Tonino et al., 2017). Titin also plays a key role as a passive elastic element based on its strategic location – extending from the middle of the M-line to the Z-line (Granzier and Labeit, 2007; Wang et al., 1993) – and structural features, enabling reversible unfolding as an entropic spring (Linke et al., 1998; Oberhauser et al., 2001; Rief et al., 1997).

However, while the importance of titin's role in muscle is beyond dispute, its functional role in bearing passive tension within muscles during normal movement remains unclear. Titin has been purported to act as a 'tunable spring' that affects muscle function (Hessel et al., 2017) and a discussion of its significance often includes its role in regulating passive mechanical properties in normal muscle (Anderson and Granzier, 2012; Granzier and Labeit, 2007). Clearly, if muscles can regulate titin to directly affect passive stiffness, it would represent a potential strategic target for therapeutic intervention. However, a number of recent studies in mammalian muscle call titin's role in functional passive load bearing into question (Meyer and Lieber, 2011; Smith et al., 2011; Wood et al., 2014). These conflicting reports suggest that the structural mechanisms that regulate passive muscle stiffness may fundamentally differ between amphibians and mammals.

Direct comparison between frog and mouse studies is complicated by the numerous ways that these properties are quantified in different studies (Table 1). Muscle tensions are reported using different units of mass (e.g. kg, oz), force (e.g. N, dynes) and are normalized to specimen size either by cross-sectional area (e.g. g cm⁻², N m⁻² or Pascals) or muscle mass (e.g. g g⁻¹ muscle mass, mg g⁻¹ body mass), depending on the study. Modulus and stiffness values are also highly dependent on the experimental approach used, especially when modulus–length relationships are nonlinear, as in composite muscle specimens such as fiber bundles and whole muscles (Lieber et al., 2003). Although literature comparisons of frog and mammalian muscle suggest that there may be species-specific differences in passive material properties (Azizi and Roberts, 2010; Brown et al., 1996), no study to date has directly compared between species using consistent testing methodology and analytical strategies to quantify the cellular and extracellular bases for any differences.

In this short report, we measured the passive modulus of muscle from two specific muscles – one in frog and one in mouse – at two size scales: frog muscle fibers ($n=14$), frog muscle fiber bundles ($n=9$), mouse muscle fibers ($n=17$) and mouse muscle fiber bundles ($n=10$). We used the same experimental protocol, instrumentation and analysis for both species to enable rigorous comparison between the mechanical properties. If titin is the primary contributor to the passive modulus, then muscle fibers and muscle fiber bundles will have similar moduli as a function of sarcomere length whereas if ECM plays a major load bearing role, fiber bundles will have a

¹Program in Physical Therapy, and Departments of Neurology, Biomedical Engineering and Orthopaedic Surgery, Washington University School of Medicine, St Louis, MO 63110, USA. ²Shirley Ryan AbilityLab and Departments of Physical Medicine and Rehabilitation, Physiology and Biomedical Engineering, Northwestern University, Chicago, IL 60611, USA.

*Author for correspondence (rlieber@sralab.org)

 G.M., 0000-0001-9268-3993; R.L.L., 0000-0002-7203-4520

Table 1. Definitions and examples of passive mechanical properties

Passive mechanical property	Definition	Examples
Passive tension	Tension (force) sustained at a given strain or sarcomere length	Anderson et al., 2001; Bensamoun et al., 2006; Prado et al., 2005
Passive stress	Passive tension divided by specimen cross-sectional area	Anderson et al., 2001; Bensamoun et al., 2006
Young's (elastic) modulus	Slope of a linear elastic stress–strain or stress–sarcomere length curve	Bensamoun et al., 2006; Lakie and Robson, 1988; Wolff et al., 2006
Regional elastic modulus	Slope of a non-linear stress–strain or stress–sarcomere length curve over a region that exhibits linearity	Magid and Law, 1985; Jewell and Wilkie, 1958; Rowe et al., 2010
Tangent modulus	Slope of a non-linear stress–strain or stress–sarcomere length curve at a given strain or sarcomere length	Smith et al., 2011; Meyer and Lieber, 2011; Wood et al., 2014
Modulus coefficient(s)	Coefficient(s) obtained by regression of a stress–strain or stress–sarcomere length curve to a nonlinear model (typically polynomial, exponential or strain–energy density functions)	Magid and Law, 1985; Best et al., 1994; Sarver et al., 2003

much larger modulus compared with single fibers and this difference will become greater with increasing sarcomere length because of the nonlinearity of ECM elasticity.

MATERIALS AND METHODS

Experiments were performed on isolated single muscle fibers and muscle fiber bundles from the anterior head of the frog [*Rana pipiens* (Schreber 1782); Carolina Biological Supply] semitendinosus muscle or on single muscle fibers and muscle fiber bundles from the 5th toe of the extensor digitorum longus (EDL) muscle of mice (*Mus musculus*, strain 129/Sv 7–9 weeks old; Taconic Farms, Germantown, NY, USA). All procedures were performed in accordance with the NIH Guide for the Use and Care of Laboratory Animals and were approved by the University of California and Department of Veteran's Affairs Committees on the Use of Animal Subjects in Research.

Details of the dissection procedures used have been described previously for both frog (Lieber and Baskin, 1983) and mouse (Meyer and Lieber, 2011; Shah and Lieber, 2003). Briefly, frog semitendinosus muscles and mouse EDL muscles were dissected and skinned overnight in a glycerinated relaxing solution. Single fibers and fiber bundles (10–20 fibers) were dissected in a chilled relaxing solution [containing (in mmol l⁻¹): EGTA (7.5), potassium propionate (170), magnesium acetate (2), imidazole (5), creatine phosphate (10) and ATP (4), with leupeptin (17 µg ml⁻¹) and E64 (4 µg ml⁻¹) to prevent protein degradation] under a stereomicroscope (MZ12.5, Leica, Deerfield, IL, USA) equipped with a transmitted light base for darkfield imaging. After dissection, one end of the specimen (frog fiber or fiber bundle; mouse fiber or fiber bundle) was attached via a 10-0 suture to a motor arm (Newport MT-RS; Irvine, CA, USA), which controlled specimen length, and the other end was attached to a force transducer (Aurora Scientific 405A; Aurora, Ontario, Canada). Sarcomere length, measured by laser diffraction using transillumination with a low

power laser diode, provided objective assessments of muscle strain and myofibrillar array quality (Lieber et al., 1984).

Passive mechanical properties were derived using an incremental stress relaxation protocol. Specimens were stretched in ~10% strain increments at 2000% per second to impose a ~0.25 µm sarcomere length change, which was maintained for 3 min to allow stress relaxation. Passive elastic properties were determined from data from fully stress-relaxed muscle with exponential fits (Fig. 1) for consistency with previously the three published analytical approaches (Azizi and Roberts, 2010; Brown et al., 1996; Magid and Law, 1985). The form of the equation was:

$$y = \frac{a}{b}(e^{bx} - 1).$$

Tangent modulus was calculated as the slope of the tangent to these curves at various sarcomere lengths and values are expressed in kPa µm⁻¹ (Table 1). This is because, for skeletal muscle, plotting stress against sarcomere length rather than strain allows physiological comparisons among muscles and species since tangent moduli at different points of the length–tension curve or sarcomere lengths at different joint angles can be investigated; this information is lost with traditional engineering normalization approaches. Typically, modulus is expressed as a ratio of stress to strain in units of kPa, which works quite well for comparisons between materials for which a zero-stress point can be reliably established and the point of desired comparison can be defined relative to that zero-stress state. In our experiments, our zero-stress point (fiber or bundle slack length) was determined by positioning the fiber such that it was visibly buckled then increasing length until the force reading on the transducer crossed a defined threshold. As

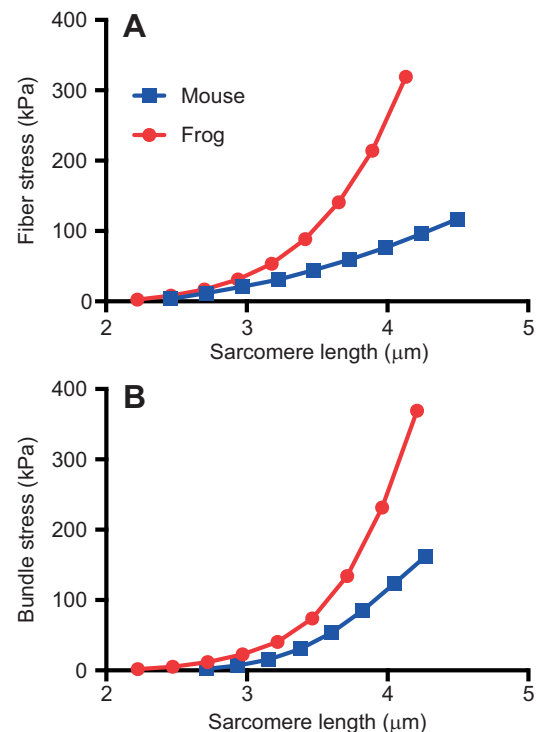


Fig. 1. Raw stress–sarcomere length curves from frog and mouse muscle. Stress versus length curves for frog and mouse single muscle fibers (A) and fiber bundles (B). Representative data from one experiment. Data are plotted in terms of sarcomere length to enable comparison across species and on different portions of the sarcomere length–tension curves.

frog fibers are both larger in cross section and stiffer than mouse, normalizing to this value could also confound our comparison.

Data were compared across species and sample type by two-way ANOVA and considered significant (α) at $P < 0.05$. Individual groups were compared using Tukey's multiple comparison test. Data are presented as means \pm s.e.m.

RESULTS AND DISCUSSION

Sarcomere length–stress relationships for all mouse single fibers tested were highly linear with $\sim 98\%$ of the experimental variation explained by a linear relationship. However, frog fibers exhibited nonlinearity in their sarcomere length–stress relationships with only $\sim 86\%$ of the experimental variation explained by the linear fit (compared to $>95\%$ with an exponential fit). To account for this nonlinearity and to enable consistent comparisons across samples, all data were fit with an exponential function. For frog muscle, modulus increased with increasing sarcomere length and was identical for fibers and bundles (Fig. 2A). However, for mouse muscle, bundle moduli diverged from fibers at a sarcomere length of about $3.2 \mu\text{m}$ and this difference became more pronounced with increasing sarcomere length, more than doubling the modulus of mouse fibers at the longest sarcomere lengths tested (Fig. 2B). As expected, two-way ANOVA comparing fibers and bundles within a species found a significant effect of sarcomere length on tangent modulus for specimens of both species ($P < 0.0001$). However, only in the mouse samples was there a significant effect of specimen type ($P < 0.01$) and a significant specimen to sarcomere length interaction ($P < 0.0001$), demonstrating different passive mechanical properties between fibers and bundles in mouse but not in frog.

Species-specific comparisons can be derived from these tangent modulus versus sarcomere length plots at a single sarcomere length, a relative position on the sarcomere length–tension curve, or a relative position in a specific muscle's sarcomere length operating range. Since the muscles used in this study were functionally different (ankle/toe dorsiflexor versus hip extensor/knee flexor), we chose to compare them at the same relative locations on their length–tension curve: 75% down the descending limb for each species ($3.47 \mu\text{m}$ for mouse; $3.21 \mu\text{m}$ for frog). At these sarcomere lengths, frog fibers were much stiffer than mouse fibers: frog modulus ($135 \pm 25 \text{ kPa } \mu\text{m}^{-1}$) exceeded mouse modulus ($42 \pm 3.7 \text{ kPa } \mu\text{m}^{-1}$) by over three-fold (Fig. 2C). Similarly, frog bundles were stiffer than mouse bundles, but the difference at these sarcomere lengths was only about 1.5-fold (Fig. 2C). This difference arises from the fact that mouse bundle moduli were around double the mouse fiber moduli, but frog bundle moduli were actually slightly lower than fiber moduli. As expected based on these observations, two-way ANOVA found a significant species \times size scale interaction ($P < 0.01$) explicitly demonstrating a species-dependent effect on scaling passive muscle tension.

This study demonstrates that the passive elastic tensile load borne by frog fibers is almost exclusively borne by the muscle fibers themselves rather than by the ECM (as demonstrated in the landmark paper of Magid and Law, 1985) while the ECM bears the majority of the passive elastic tensile load in mouse fiber bundles, with a ratio of ECM:muscle fiber load bearing of about 55:45 at a sarcomere length of $3.47 \mu\text{m}$ (Fig. 3). The calculations are based on the area fraction of ECM and muscle fibers (A_f) as well as the moduli of the ECM (E_m) and fibers (E_f) structures as previously reported (Meyer and Lieber, 2012). This calculation was made by assuming that bundle, fiber and matrix strain are all identical. Then, using the definition of stress, and the law of mixtures, load borne by

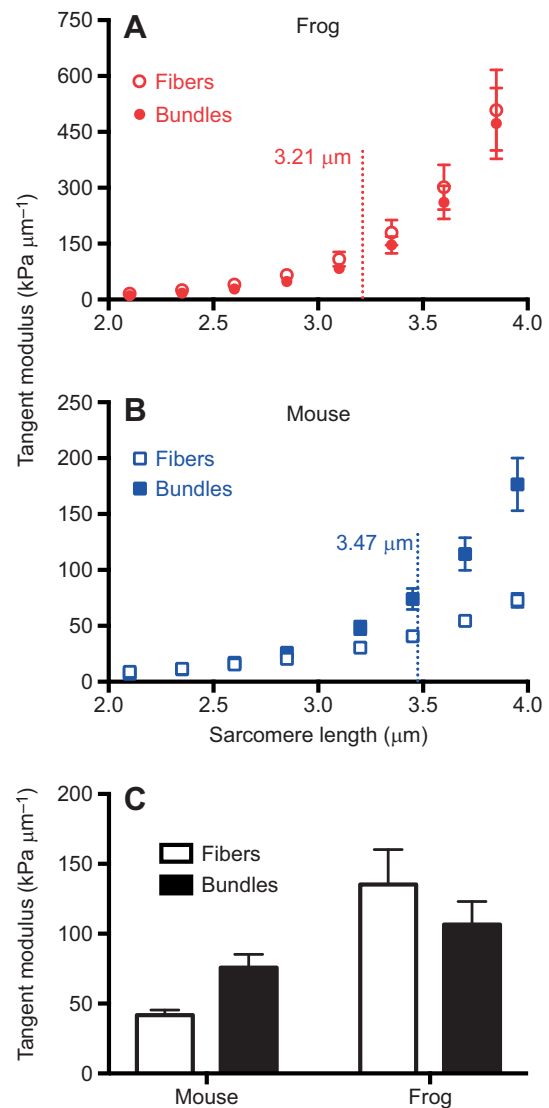


Fig. 2. Tangent modulus for frog and mouse fibers and bundles as a function of sarcomere length. Tangent modulus for fibers and bundles in frog (A) and mouse (B) as a function of sarcomere length. Tangent moduli were calculated at sarcomere lengths across the plateau and descending limb of the length–tension curve for each species in $0.25 \mu\text{m}$ increments (means \pm s.e.m., $n = 9–17$ per group). Vertical dotted line is placed at the species-specific 75% point on the descending limb and this value is plotted in C. (C) Modulus values from frog and mouse single fibers and fiber bundles at the sarcomere length denoted by vertical dotted lines in A and B. Two-way ANOVA found a significant species \times size scale interaction ($P < 0.01$) explicitly demonstrating a species-dependent effect on scaling of passive tension (means \pm s.e.m., $n = 9–17$ per group).

the matrix (F_m) relative to load borne by fibers (F_f) is:

$$\frac{F_m}{F_f} = \frac{E_m}{E_f} \times \frac{(1 - A_f)}{(A_f)}$$

In contrast, this calculation predicts that frog fibers bear nearly all of the passive load at a sarcomere length of $3.21 \mu\text{m}$ (the same relative position on their length–tension curve as mouse; Fig. 3) assuming a similar area fraction of ECM and muscle fibers. Furthermore, the coefficient b , which represents the curvature of the exponential data, is significantly higher in mouse bundles (1.73 ± 0.06) compared with mouse fibers (1.16 ± 0.05), but is not significantly different between

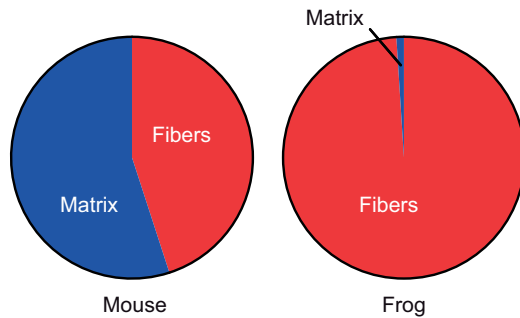


Fig. 3. Fraction of passive load borne by frog and mouse muscle fibers.

Values are predicted by the rule of mixtures assuming these muscles are a continuous composite of 90% unidirectional fibers and 10% extracellular matrix (Meyer and Lieber, 2012) using the fiber and bundle moduli presented in this report.

frog bundles (2.26 ± 0.15) and frog fibers (2.03 ± 0.15). This indicates that not only the tangent stiffness but also the nonlinearity of the passive stress–sarcomere length relationship in frogs is dominated by the fibers (consistent with the landmark paper of Magid and Law, 1985). This is clearly not the case for mouse muscle.

These data from frog and mouse reflect different distributions of passive load bearing between species, with frog muscle relying almost solely on fibers and mouse distributing passive tensile load between fibers and the surrounding ECM. The structural basis for these differences could lie either in titin or the ECM. Frog isoforms of titin may be shorter (and therefore stiffer) and more non-linearly elastic than mouse. On the other hand, frog muscle may have a more integrated endomysium that remains with dissected individual fibers and bears a portion of passive tension. While the teleological explanation is unclear, these results are unsurprising to researchers who have attempted to dissect intact single cells from both species. While intact frog single fiber dissections are challenging, they are easily learned with practice. In contrast, the only mouse muscle for which intact fibers can be reliably dissected is the intrinsic muscle of the foot, the flexor digitorum brevis (FDB) muscle, which has a very low connective tissue content. Even so, partial collagen digestion with collagenase is required to free muscle fibers from the ECM without mechanical damage (Cheng and Westerblad, 2017).

It has been demonstrated in mammalian muscle cells, that titin bears from 10 to 50% of single fiber tension (Prado et al., 2005). Since we show here that mammalian fibers bear about 45% of bundle tension (Fig. 3), this leads to the conclusion that titin bears at most about 22.5% of fiber bundle tension (50% of 45%). Scaling the results of this study to whole muscle properties is complicated by various levels of fiber and ECM organization. However, the perimysium with its larger quantities of connective tissue and unique collagen ultrastructure (Gillies and Lieber, 2011) likely increases the role of the ECM in passive whole muscle loadbearing. Literature reports of increased passive stiffness in mammalian muscle compared with frog (Azizi, 2014; Brown et al., 1996) are consistent with this hypothesis. Although we find that frog fibers are substantially stiffer than mouse, most of this difference is eliminated at the bundle level. We predict that at higher levels of mammalian muscle organization the contribution of the ECM will supersede that of the fibers. In support of this, our recent report that fiber bundles bear only 5–10% of the passive stiffness of whole muscles (T. M. Winters and S. R. Ward, personal communication) implies that titin would bear only 1–2% of whole muscle tension in mammalian muscle (5–10% of 22.5%), which is not likely to be functionally important, even if titin stiffness changed by orders of magnitude.

Taken together, these experiments contradict the hypothesis that titin is functionally load bearing at the whole muscle level in mammalian skeletal muscle.

It should be noted that these arguments are only valid, strictly speaking, for these specific mouse and frog muscles. While other measurements of frog and mouse muscle are consistent with these findings, the strict comparison can only be made for these two muscles. It has been shown that, for whole muscles, passive mechanical properties can vary within a species (Azizi, 2014; Brown et al., 1996) but the structural basis for this observation is not known. It is clear that skeletal muscles among species can use a variety of strategies to modulate passive mechanical properties and these strategies are related in some way, to that particular muscle's function.

Acknowledgements

We appreciate the persistent and thoughtful comments made by the reviewers to improve the clarity and impact of this work.

Competing interests

The authors declare no competing or financial interests.

Author contributions

Conceptualization: G.M., R.L.L.; Methodology: G.M., R.L.L.; Software: G.M.; Validation: G.M.; Formal analysis: G.M., R.L.L.; Investigation: G.M.; Data curation: G.M., R.L.L.; Writing - original draft: R.L.L.; Writing - review & editing: G.M., R.L.L.; Visualization: G.M., R.L.L.; Supervision: R.L.L.; Project administration: R.L.L.; Funding acquisition: R.L.L.

Funding

This work was supported by the National Institutes of Health (R01 AR40050 and R24 HD050837 to R.L.L.), and the Department of Veterans Affairs (R.L.L.). Deposited in PMC for release after 12 months.

References

- Anderson, J., Li, Z. and Goubel, F. (2001). Passive stiffness is increased in soleus muscle of desmin knockout mouse. *Muscle Nerve* **24**, 1090–1092.
- Anderson, B. R. and Granzier, H. L. (2012). Titin-based tension in the cardiac sarcomere: molecular origin and physiological adaptations. *Prog. Biophys. Mol. Biol.* **110**, 204–217.
- Azizi, E. (2014). Locomotor function shapes the passive mechanical properties and operating lengths of muscle. *Proc. Biol. Sci.* **281**, 20132914.
- Azizi, E. and Roberts, T. J. (2010). Muscle performance during frog jumping: influence of elasticity on muscle operating lengths. *Proc. Biol. Sci.* **277**, 1523–1530.
- Bensamoun, S., Stevens, L., Fleury, M. J., Bellon, G., Goubel, F. and Ho Ba Tho, M. C. (2006). Macroscopic-microscopic characterization of the passive mechanical properties in rat soleus muscle. *J. Biomech.* **39**, 568–578.
- Best, T. M., McElhaney, J., Garrett, W. E., Jr and Myers, B. S. (1994). Characterization of the passive responses of live skeletal muscle using the quasi-linear theory of viscoelasticity. *J. Biomech.* **27**, 413–419.
- Brown, I. E., Liinamaa, T. L. and Loeb, G. E. (1996). Relationships between range of motion, l_0 , and passive force in five strap-like muscles of the feline hind limb. *J. Morphol.* **230**, 69–77.
- Cheng, A. J. and Westerblad, H. (2017). Mechanical isolation, and measurement of force and myoplasmic free $[Ca^{2+}]$ in fully intact single skeletal muscle fibers. *Nat. Protoc.* **12**, 1763–1776.
- Edman, K. A. P. (1966). The relation between sarcomere length and active tension in isolated semitendinosus fibres of the frog. *J. Physiol.* **183**, 407–417.
- Edman, K. (1979). The velocity of unloaded shortening and its relation to sarcomere length and isometric force in vertebrate muscle fibres. *J. Physiol.* **246**, 255–275.
- Gillies, A. M. and Lieber, R. L. (2011). Structure and function of the skeletal muscle extracellular matrix. *Muscle Nerve* **44**, 318–331.
- Gordon, A. M., Huxley, A. F. and Julian, F. J. (1966a). Tension development in highly stretched vertebrate muscle fibres. *J. Physiol.* **184**, 143–169.
- Gordon, A. M., Huxley, A. F. and Julian, F. J. (1966b). The variation in isometric tension with sarcomere length in vertebrate muscle fibres. *J. Physiol.* **184**, 170–192.
- Granzier, H. and Labeit, S. (2007). Structure-function relations of the giant elastic protein titin in striated and smooth muscle cells. *Muscle Nerve* **36**, 740–755.
- Hessel, A. L., Lindstedt, S. L. and Nishikawa, K. C. (2017). Physiological mechanisms of eccentric contraction and its applications: a role for the giant titin protein. *Front. Physiol.* **8**, 70.

- Hill, A. V. (1938). The heat of shortening and the dynamic constants of muscle. *Proc. R. Soc. Lond. Series B Biol. Sci.* **126**, 136-195.
- Hill, A. V. (1953). The mechanics of active muscle. *Proc. R. Soc. Lond. Series B Biol. Sci.* **141**, 104-117.
- Horowitz, R., Kempner, E. S., Bisher, M. E. and Podolsky, R. J. (1986). A physiological role for titin and nebulin in skeletal muscle. *Nature (Lond.)* **323**, 160-164.
- Jewell, B. R. and Wilkie, D. R. (1958). An analysis of the mechanical components in frog's striated muscle. *J. Physiol.* **143**, 515-540.
- Knöll, R., Hoshijima, M., Hoffman, H. M., Person, V., Lorenzen-Schmidt, I., Bang, M.-L., Hayashi, T., Shiga, N., Yasukawa, H., Schaper, W. et al. (2002). The cardiac mechanical stretch sensor machinery involves a Z disc complex that is defective in a subset of human dilated cardiomyopathy. *Cell* **111**, 943-955.
- Labeit, S. and Kolmerer, B. (1995). Titins: Giant proteins in charge of muscle ultrastructure and elasticity. *Science* **270**, 293-296.
- Lakie, M. and Robson, L. G. (1988). Thixotropy: the effect of stretch size in relaxed frog muscle. *Q. J. Exp. Physiol.* **73**, 127-129.
- Lange, S., Xiang, F., Yakovenko, A., Vihola, A., Hackman, P., Rostkova, E., Kristensen, J., Brandmeier, B., Franzen, G., Hedberg, B. et al. (2005). The kinase domain of titin controls muscle gene expression and protein turnover. *Science* **308**, 1599-15603.
- Lieber, R. L. and Baskin, R. J. (1983). Intersarcomere dynamics of single muscle fibers during fixed-end tetani. *J. Gen. Physiol.* **82**, 347-364.
- Lieber, R. L., Yeh, Y. and Baskin, R. J. (1984). Sarcomere length determination using laser diffraction. Effect of beam and fiber diameter. *Biophys. J.* **45**, 1007-1016.
- Lieber, R. L., Runesson, E., Einarsson, F. and Fridén, J. (2003). Inferior mechanical properties of spastic muscle bundles due to hypertrophic but compromised extracellular matrix material. *Muscle Nerve* **28**, 464-471.
- Linke, W. A., Stockmeier, M. R., Ivemeyer, M., Hosser, H. and Mundel, P. (1998). Characterizing titin's I-band Ig domain region as an entropic spring. *J. Cell Sci.* **111**, 1567-1574.
- Magid, A. and Law, D. J. (1985). Myofibrils bear most of the resting tension in frog skeletal muscle. *Science* **230**, 1280-1282.
- Maruyama, K., Sawada, J., Kimura, S., Ohashi, K., Higuchi, H. and Umazume, Y. (1984). Connectin filaments in stretched skinned fibers of frog skeletal muscle. *J. Cell Biol.* **99**, 1391-1397.
- Meyer, G. A. and Lieber, R. L. (2011). Elucidation of extracellular matrix mechanics from muscle fibers and fiber bundles. *J. Biomech.* **44**, 771-773.
- Meyer, G. A. and Lieber, R. L. (2012). Skeletal muscle fibrosis develops in response to desmin deletion. *Am. J. Physiol. Cell Physiol.* **302**, C1609-C1620.
- Oberhauser, A. F., Hansma, P. K., Carrion-Vazquez, M. and Fernandez, J. M. (2001). Stepwise unfolding of titin under force-clamp atomic force microscopy. *Proc. Natl. Acad. Sci. USA* **98**, 468-472.
- Prado, L. G., Makarenko, I., Andresen, C., Kruger, M., Opitz, C. A. and Linke, W. A. (2005). Isoform diversity of giant proteins in relation to passive and active contractile properties of rabbit skeletal muscles. *J. Gen. Physiol.* **126**, 461-480.
- Rief, M., Gautel, M., Oesterhelt, F., Fernandez, J. M. and Gaub, H. E. (1997). Reversible unfolding of individual titin immunoglobulin domains by AFM. *Science* **276**, 1109-1112.
- Rowe, J., Chen, Q., Domire, Z. J., McCullough, M. B., Sieck, G., Zhan, W.-Z. and An, K.-N. (2010). Effect of collagen digestion on the passive elastic properties of diaphragm muscle in rat. *Med. Eng. Phys.* **32**, 90-94.
- Sarver, J. J., Robinson, P. S. and Elliott, D. M. (2003). Methods for quasi-linear viscoelastic modeling of soft tissue: application to incremental stress-relaxation experiments. *J. Biomech. Eng.* **125**, 754-758.
- Shah, S. B. and Lieber, R. L. (2003). Simultaneous imaging and functional assessment of cytoskeletal protein connections in passively loaded single muscle cells. *J. Histochem. Cytochem.* **51**, 19-29.
- Smith, L. R., Lee, K. S., Ward, S. R., Chambers, H. G. and Lieber, R. L. (2011). Hamstring contractures in children with spastic cerebral palsy result from a stiffer extracellular matrix and increased in vivo sarcomere length. *J. Physiol.* **589**, 2625-2639.
- Tonino, P., Kiss, B., Strom, J., Methawasin, M., Smith, J. E., III, Kolb, J., Labeit, S. and Granzier, H. (2017). The giant protein titin regulates the length of the striated muscle thick filament. *Nat. Commun.* **8**, 1041.
- Wang, K., McCarter, R., Wright, J., Beverly, J. and Ramirez-Mitchell, R. (1993). Viscoelasticity of the sarcomere matrix of skeletal muscles. The titin-myosin composite filament is a dual-stage molecular spring. *Biophys. J.* **64**, 1161-1177.
- Wolff, A. V., Niday, A. K., Voelker, K. A., Call, J. A., Evans, N. P., Granata, K. P. and Grange, R. W. (2006). Passive mechanical properties of maturing extensor digitorum longus are not affected by lack of dystrophin. *Muscle Nerve* **34**, 304-312.
- Wood, L. K., Kayupov, E., Gumucio, J. P., Mendias, C. L., Clafin, D. R. and Brooks, S. V. (2014). Intrinsic stiffness of extracellular matrix increases with age in skeletal muscles of mice. *J. Appl. Physiol.* **117**, 363-369.